

# Optimal Computation-Communication Trade-offs in Processing Networks

Luca Ballotta, Luca Schenato, Luca Carlone

**Abstract**—This paper investigates the use of a networked system (e.g., swarm of robots, smart grid, sensor network) to monitor a time-varying phenomenon of interest in the presence of communication and computation latency. Recent advances on edge computing are enabling processing to be performed at each sensor, hence we investigate the fundamental *latency-accuracy trade-off*, arising when a sensor in the network has to decide whether to transmit raw data (incurring a computational delay) or transmit it (incurring communication delays) in order to compute an accurate estimate of the state of the phenomenon of interest. We propose two key contributions. First, we formalize the notion of *processing network*. Contrarily to *sensor and communication networks*, where the designer is concerned with the design of a suitable communication policy, in a *processing network* one can also control when and where the computation occurs in the network. The second contribution is to provide analytical results on the optimal communication latency (i.e., the optimal time spent on processing at each node) for the case with a single sensor and multiple homogeneous sensors. Numerical results substantiate our claims that accounting for computation and communication delays can largely impact the estimation accuracy, and the latency-accuracy trade-off becomes even more relevant in the presence of bandwidth constraints, large networks, and limited computational resources.

**Index Terms**—Networked systems, Communication latency, processing latency, processing network, resource allocation, sensor fusion, smart sensors.

## I. INTRODUCTION

Networked systems are becoming an ubiquitous technology across many application domains, including city-wide air-pollution monitoring [16], smart power grids [22], swarms of mobile robots for smart farming and supply chain logistics [2], [15], interconnected autonomous vehicles and self-driving cars [25]. Progress on communication systems, such as the development of 5G, carries the promise of further expanding the reach of these systems by enabling more effective and larger-scale deployments. At the same time, recent advances on embedded computing, from embedded GPU-CPU systems [19] to specialized hardware [26], are now providing unprecedented opportunities for *edge-computing*, where sensor data is processed locally at the sensor to minimize the communication burden.

The availability of powerful embedded computers creates a nontrivial *latency-accuracy trade-off*: is it best to transmit raw sensor data and incur larger communication and data fusion delays at a central station, or to perform more preprocessing

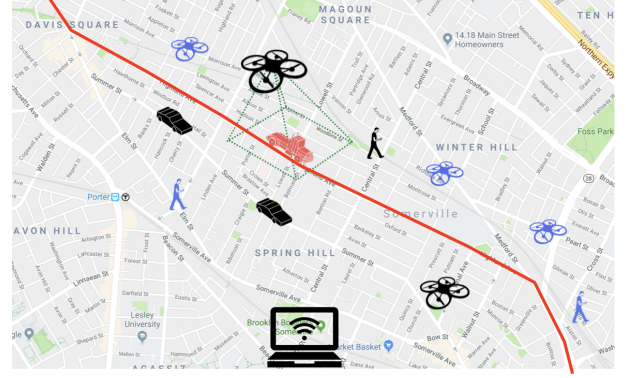


Figure 1: Example of a *processing network* (smart sensors shown in blue and black) tracking the state of the vehicle in red in the presence of communication and computational latency.

at the sensors and transmit more refined (less noisy and more compressed) estimates? Fig. 1 provides an example of this trade-off: the figure depicts a network of *smart sensors* (in black and blue) observing and tracking the state of a moving vehicle (in red) and transmitting data to a central fusion station (the computer at the bottom of the figure), which is in charge of monitoring the state of the red truck. The smart sensors may have heterogeneous computational resources: for instance, the large drone (in black) might have a powerful onboard GPU-CPU system, while other smart sensors (in blue, e.g., smaller drones, mobile phones) might have limited computation. Therefore, some sensors might prefer sending raw data and incur more delay when transmitting the data, while some other sensors might prefer preprocessing the data at the edge. These choices will impact the quality of the red vehicle estimate: larger computation and computation delays will lead to less accurate estimates, hindering the tracking task.

In this paper we investigate the latency-accuracy trade-off that arises in a networked system responsible for estimating the state of a time-varying phenomenon of interest in the presence of computation and communication delays. Related work in the IoT community focuses on optimizing data transmission by means of smart communication policies, with respect to estimation performance [37] or the so-called *Age of Information* (AoI) due to latency and unreliability [38], [39], [41]. Contrary to this line of work, we focus on monitoring a dynamical system and advocate a unified task-driven framework, where computation and communication are jointly modeled in an optimal estimation framework. In hindsight, we propose a paradigm shift from *sensor and communication networks*, in

L. Ballotta and L. Schenato are with the Department of Information Engineering, University of Padova, University of Padova, Padova, 35131, Italy (e-mail: {ballotta, schenato}@dei.unipd.it).

L. Carlone is with Institute for Data, Systems and Society, and the Laboratory for Information & Decision Systems, Massachusetts Institute of Technology, Boston, 02139, USA (e-mail: lcarlone@mit.edu).

which one has to decide the best communication policy, to *processing networks*, where one also controls when and where the computation occurs. Also, we establish quantitative connections among latency, system dynamics and estimation performance, while abovementioned works are more qualitative-oriented.

Related work in control, cyber-physical systems, and robotics focuses on either the co-design of estimation and control in the presence of communication constraints [1], [3], [8], [17], [21], [23], [24], [32], or on the design of the system's sensing and actuation [5], [6], [9], [12]–[14], [18], [20], [27]–[29], [35], [40]. [31] and [34] establish a more direct connection between sensing and estimation performance, by proposing co-design approaches for sensing, estimation, and control. While these works focus on communication constraints, we attempt to explicitly model *computation delays* and understand how they impact the performance of the estimation task. [7] adopt a learning approach for computational-offloading in cloud-robotics applications. [36] and [4] investigate the performance of drone teams in a wireless sensor network. [33] seeks a policy to tackle edge-computing latency within a static framework. Other work is about modeling and analysis: [30] characterize performance of resource-constrained devices with cloud fog offloading (with case study on FFT computation), while [11] investigate multimedia data processing within pipeline and parallel architectures. Contrary to these works, we consider a dynamical system, we explicitly model communication and computational latency, and we are concerned with the derivation of optimal computation and communication policies for estimation.

We propose the following contributions. First, we formalize the notion of processing network and provide a model which is amenable for analysis (Section II). The networked system is modeled as a set of smart sensors in charge of estimating the state of a dynamical system in the presence of communication and computation latency. Edge devices run so-called *anytime algorithms*, *i.e.*, performing better according to longer runtime. The key idea is to capture such *anytime* nature of the preprocessing using a processing-dependent measurement noise at each sensor. Second, we derive fundamental limits for such model: we prove that in two instantiations of the model there is an optimal choice for the amount of preprocessing done at each node, which can be computed analytically in the case with scalar-state homogeneous-sensor networks. Numerical simulations confirm that such trend is still valid for multidimensional systems. Third, we go through heterogeneous networks and extend the optimization problem so as to account for both optimal sensor subset and preprocessing delay selection. Such problem is combinatorial and therefore we propose greedy algorithms to deal with it. In particular, Section III introduces the problem within homogeneous, continuous-time, scalar networks, which is extended to general homogeneous networks in Section IV. Section V presents the wider heterogeneous-network framework: while the model is presented in detail in Subsection V-A, Subsection V-B we describe an iterative algorithm to compute the cost function. The greedy selection algorithms are proposed in Section VI, while a numerical experiment is presented in Section VII

to assess their performance. Finally, conclusions are drawn in VIII together with possible future works.

## II. ESTIMATION IN PROCESSING NETWORKS: PROBLEM FORMULATION

A *processing network* is a set of interconnected *smart sensors* that collect sensor data and leverage onboard computation to locally preprocess the data before communicating it to a central fusion center. The goal of the network is to obtain an accurate estimate of the state of a time-varying phenomenon observed by the sensors, in the face of communication and computation latencies.

### A. Anatomy of a Processing Network

**Dynamical system:** We consider a processing network monitoring a time-varying phenomenon described by the following linear time-invariant (LTI) stochastic model:

$$dx_t = A x_t dt + dw_t \quad (1)$$

where  $x_t \in \mathbb{R}^n$  is the to-be-estimated state of the system at time  $t$ ,  $A \in \mathbb{R}^n$  is a constant describing the system dynamics, and  $w_t \sim (0, Q)$  represents process noise. We start with the scalar sub-case of (1), which can be analyzed analytically, and address the multi-variate case in Subsection IV-A.

**Smart sensors:** The processing network includes  $N$  smart sensors,  $\mathcal{N} = \{1, \dots, N\}$ . After acquiring data, each sensor may refine raw measurements via some local preprocessing. For instance, in the robotics application of Fig. 1, each robot is a smart sensor that may process raw data (e.g., images) to obtain local measurements of the state (e.g., the tracked vehicle location in Fig. 1). Depending on the time and computational resources, the robot may use more sophisticated algorithms (or a larger number of visual features [10]) to obtain more accurate measurements. More generally, the use of *anytime algorithms* [42] at each sensor entails a trade-off, where the more time is spent on preprocessing, the more accurate is the measurement by the sensor. We capture the dependence of the measurements (and their noise) on the preprocessing time through the following model:

$$z_t(\tau_p) = Cx_t + v_t(\tau_p), \quad z_t(\tau_p) = \begin{bmatrix} z_t^{(1)}(\tau_{p,1}) & \dots & z_t^{(N)}(\tau_{p,N}) \end{bmatrix}^T \quad (2)$$

where  $z_t^{(i)} \in \mathbb{R}^{m_i}$  is the measurement collected at time  $t$  by the  $i$ -th sensor,  $\tau_{p,i}$  is the *preprocessing delay* associated with the  $i$ -th sensor, and  $v_t$  is white noise;  $\tau_p \doteq \{\tau_{p,i}\}_{i \in \mathcal{N}}$ , and  $z_t$  contain the delays and measurements from all sensors. In order to capture the anytime nature of the sensor preprocessing, we model the intensity of the white noise  $v_t$  as a decreasing function of  $\tau_p$  (see Section III).

**Communication:** The sensors send preprocessed data to the central station for data fusion. To simplify the mathematical analysis, we assume what follows.

**Assumption 1** (Reliable channel). Packet loss and channel erasure probabilities are equal to zero.

Given limited bandwidth, also data transmission induces a *communication delay*  $\tau_{c,i}$  for each sensor  $i$ . In addition to

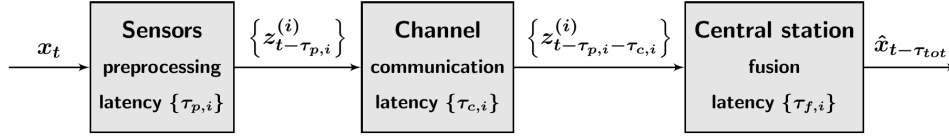


Figure 2: Block diagram of the processing network with latency contributions by preprocessing, communication and fusion.

Assumption 1, we assume unconstrained channel capacity, so that all sensors can transmit “in parallel”. We then consider two models for  $\tau_{c,i}$  as a function of  $\tau_{p,i}$ :

- *constant*  $\tau_{c,i}$ : the transmitted packet length/number is fixed and does not depend on the preprocessing; in this case the communication delay is a constant, irrespective of the preprocessing delay  $\tau_{p,i}$ .
- *decreasing*  $\tau_{c,i}$ : in this case, sensor preprocessing *compresses* the measurements, such that a longer preprocessing leads to less packets to transmit.

**Fusion center:** The central station is in charge of fusing all sensor data to compute a state estimate. We assume that  $\mathcal{Z}_t(\tau_p) = \{z_{s_i}^{(i)}(\tau_{p,i}), s_i \in [t_0, t - \tau_{p,i} - \tau_{c,i}]\}_{i \in \mathcal{N}}$  is the dataset available at time  $t$  (starting from an initial time  $t_0$ ). Fusion adds further latency, namely the *fusion delay*  $\tau_{f,tot}$ , which is the sum of the latency  $\tau_{f,i}$  required to process the data stream from each sensor  $i$ . In particular, as above, we assume that either  $\tau_{f,i}$  is constant, or it decreases with the preprocessing delay  $\tau_{p,i}$  (intuitively, the more preprocessing is done at the sensor, the less effort is needed for fusion). Fig. 2 gives an insight on the processing network with the different latency contributions - by sensor preprocessing, communication, and central station fusion.

### B. Optimal Estimation in Processing Networks

While the sensor data might be received and fused with some (computation and communication) delay, we are interested in obtaining an accurate state estimate at the current time  $t$ ; this entails fusing sensor information  $\mathcal{Z}_t(\tau_p)$  (partially outdated, due to the computation and communication delays) with the open-loop system prediction in (1). This raises a nontrivial communication-computation trade-off: is it best to transmit raw sensor data and incur larger communication and fusion delays, or to perform more preprocessing at the edge and transmit more refined (less noisy and more compressed) estimates? For instance, consider again Fig. 1 where robots compute local estimations from images. Each extracted feature both enhances sensor-side accuracy and possibly reduces transmission and fusion latency. However, feature extraction comes with preprocessing (edge computation) latency. A trade-off emerges: on one hand, many features cause a long prediction; on the other hand, few provide a poor estimation. An *optimal estimation* policy would decide the preprocessing at each sensor in a way to maximize the final estimation accuracy. Also, the fusion latency puts a constraint on the very active sensor set  $\mathcal{S} \subseteq \mathcal{N}$ . The open-loop prediction stretches with each sensor contribution  $\tau_{f,i}$ : thus, since sensors cannot be added arbitrarily without dropping the performance after a certain amount is hit, an optimal sensor subset  $\mathcal{S}_{opt}$  should be picked

out of  $\mathcal{N}$  in order to maximize the estimation performance. Such selection yields that only some of the available data are exploitable for estimation,  $\mathcal{Z}_t(\mathcal{S}, \tau_p^S) \subseteq \mathcal{Z}_t(\tau_p)$ , where  $\tau_p^S$  are the active-sensor delays. A more formal motivation about that is presented in Subsection III-B.

**Problem formulation:** In general, one may wish to optimize the estimation performance at all times, *i.e.*, as for Mean Squared Error (MSE) estimators, find  $\arg \min_{\tau_p \in \mathbb{R}_+^N} \text{var}(x_t - \hat{x}_t(\tau_p))$ , where  $\hat{x}_t(\tau_p) \doteq g(\mathcal{Z}_t(\tau_p))$  is a state estimator. However, such problem comes with the nuisance of time variance. Instead, we resort to its time-invariant steady-state counterpart by exploiting communication reliability (Assumption 1).

**Problem 1.** Given system (1) with sensor set  $\mathcal{N}$  and measurement model (2), find the optimal sensor subset and preprocessing delays that minimize the steady-state estimation error variance:

$$\begin{aligned} & \arg \min_{\substack{S \subseteq \mathcal{N} \\ \tau_p^S = \{\tau_{p,i}\}_{i \in S} \in \mathbb{R}_+^S}} \text{trace}(P_{\infty|\infty-\tau_{tot}}(\tau_p)) \end{aligned} \quad (3)$$

where  $S = |\mathcal{S}|$ , the total delay is

$$\tau_{tot} \doteq \underbrace{\max_{i \in S}(\tau_{p,i} + \tau_{c,i})}_{\doteq \tau_s} + \underbrace{\sum_{i \in S} \tau_{f,i}}_{\doteq \tau_{f,tot}} \quad (4)$$

and  $P_{\infty|\infty-\tau_{tot}}(\tau_p) \doteq \lim_{t \rightarrow +\infty} \text{var}(x_t - \hat{x}_t(\tau_p))$  is the steady-state estimation error variance.  $\tau_{tot}$  accounts for the fact that, due to delays, the steady-state estimate relies on partially outdated measurements:  $\tau_s$  is the time it takes to collect measurements from all sensors, while  $\tau_{f,tot}$  is the time it takes to fuse them.

We start by analyzing the single-sensor case to gain some intuition on Problem 1. In the following, to keep notation more readable, we drop the subscripts from the preprocessing delay  $\tau_{p,i}$  and refer to it as  $\tau$ .

### III. A GENTLE START: HOMOGENEOUS NETWORK WITH CONTINUOUS-TIME SCALAR SYSTEM

In order to get some intuition about the more realistic and general framework, we start with the simple - and analytically tractable - continuous-time, scalar case. We consider an homogeneous network with  $N$  identical sensors, thus with equal preprocessing, communication and fusion delays. For now we neglect optimization with respect to the sensors (addressed within the general scenario, see Section V), and focus on the

optimal preprocessing delay. We therefore consider system (1) with  $A \in \mathbb{R}$ :

$$dx_t = ax_t dt + dw_t \quad (5)$$

where  $x_t \in \mathbb{R}$  is the time-indexed state of the system,  $a \in \mathbb{R}$  is a constant describing its dynamics and  $w_t \sim (0, \sigma_w^2)$  is the scalar-valued, white process noise. As for the measuring system, we take the following special case of (2):

$$z_t(\tau) = (\mathbb{1}_N \otimes \tilde{C})x_t + v_t(\tau) \quad \mathbb{1}_N = \underbrace{[1, \dots, 1]^T}_{N \text{ times}} \quad (6)$$

where  $\tau \in \mathbb{R}_+$  is the preprocessing delay,  $\tilde{C}$  is a column matrix with  $m$  rows,  $z_t \in \mathbb{R}^{Nm}$  and  $v_t(\tau) \sim (0, I_N \otimes R(\tau))$  is the preprocessing noise with intensity

$$R(\tau) = \frac{b}{\tau} I_N \quad (7)$$

where for sake of simplicity we take independent sensors. Choosing the variance of preprocessing noise inversely proportional to the computation delay  $\tau$  is motivated by the observation that the variance of least squares estimation is inversely proportional to the number of data points (e.g., features extracted from an image), if these are mutually uncorrelated. Communication and fusion latency for each sensor are denoted as  $\tau_c(\tau)$  and  $\tau_f(\tau)$ , respectively, and the total gathered delay (4) boils down to

$$\tau_{tot} = \underbrace{\tau + \tau_c(\tau)}_{\tau_s} + \underbrace{\tau_f(\tau)N}_{\tau_{f,tot}} \quad (8)$$

According to the model, it holds

$$\begin{cases} \tau_c(\tau) \equiv \tau_c \\ \tau_f(\tau) \equiv \tau_f \end{cases} \quad (9) \quad \text{or} \quad \begin{cases} \tau_c(\tau) = \frac{c}{\tau} \\ \tau_f(\tau) = \frac{f}{\tau} \end{cases} \quad (10)$$

with constant or  $\tau$ -varying latency, respectively. All coefficients  $\tau_c$ ,  $\tau_f$ ,  $c$  and  $f$  are assumed to be positive, known constants<sup>1</sup>.

We rephrase Problem 1 so as to fit the current set-up:

**Problem 2** (Continuous-time homogeneous network). Given system (5) with  $N$  sensors and measurement model (6), find the optimal preprocessing delay that minimizes the steady-state estimation error variance:

$$\arg \min_{\tau \in \mathbb{R}_+} p_{\infty|\infty-\tau_{tot}}(\tau) \quad (11)$$

*Remark 1.* Notice that the proposed model for the homogeneous network is equivalent to a single sensor with noise variance  $\sigma_w^2(\tau)$  reduced by a factor  $N$  with respect to each sensor in the network, and total delay (8). The following result indeed holds the same for both such cases, provided suitable rescaling of sensor parameters.

It turns out that such problem has a unique solution, as formalized by the following theorem.

**Theorem 1** (Optimal preprocessing for continuous-time homogeneous network). *Consider the LTI scalar system (5)–(6) with*

<sup>1</sup>Such assumption may be satisfied as soon as communication and fusion delays are estimated/learned from data or a physical model.

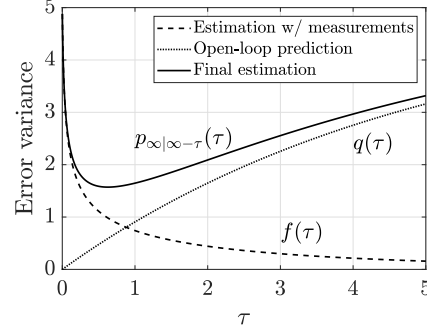


Figure 3: Visual representation of  $p_{\infty|\infty-\tau_{tot}}(\tau)$ , with contributions due to estimation  $f(\tau)$  and process noise  $q(\tau)$ .

measurement noise variance  $R(\tau)$  as per (7), communication and fusion latency  $\tau_c(\tau)$ ,  $\tau_f(\tau)$  as per (9) or (10) and initial condition  $x_{t_0} \sim (\mu_0, p_0)$ . Assume  $\hat{x}_t(\tau)$  is the Kalman filter estimate at time  $t$  given measurements collected until time  $t - \tau$ . Then, the steady-state error variance  $p_{\infty|\infty-\tau_{tot}}(\tau)$  has expression

$$p_{\infty|\infty-\tau_{tot}}(\tau) = \underbrace{e^{2a\tau_{tot}} p_{\infty}(\tau)}_{f(\tau)} + \underbrace{\frac{\sigma_w^2}{2a} (e^{2a\tau_{tot}} - 1)}_{q(\tau)}$$

where

$$p_{\infty}(\tau) = \frac{\tilde{b}}{\tau} \left( a + \sqrt{a^2 + \frac{\sigma_w^2}{\tilde{b}} \tau} \right) \quad \tilde{b} \doteq \frac{b}{N\gamma} \quad \gamma \doteq \sum_{i=1}^m (\tilde{C})_{i,1}^2$$

with limits

$$\lim_{\tau \rightarrow 0^+} p_{\infty|\infty-\tau_{tot}}(\tau) = \lim_{\tau \rightarrow +\infty} p_{\infty|\infty-\tau_{tot}}(\tau) = \begin{cases} +\infty, & a \geq 0 \\ \frac{\sigma_w^2}{2|a|}, & a < 0 \end{cases} \quad (12)$$

and a unique point of global minimum  $\tau_{opt} > 0$ .

*Proof.* See Appendix A.  $\square$

Fig. 3 illustrates the cost function of Theorem 1, together with the contributions due to projecting in open-loop the measurement-based estimation and the process noise ( $f(\tau)$  and  $q(\tau)$ , respectively). Fig. 4 compares the steady-state error variance with the two models for communication and fusion latency (dashed for constant and solid for  $\tau$ -varying) for an unstable and an asymptotically stable systems. Notice that the steepness of the dashed curve decreasing portion suggests that it is preferable to round  $\tau_{opt}$  in excess, if needed, as in this case a lower approximation likely worsens performance. Also, notice that the curves cross: the model with no/constant compression is outperformed by the  $\tau$ -varying one as soon as the preprocessing runtime exceeds a certain threshold.

*Remark 2.* While the models in (10) are mainly used for mathematical convenience, in a real setup the compression functions should be learned or estimated from data.

**Example: Brownian systems.** An interesting case arises

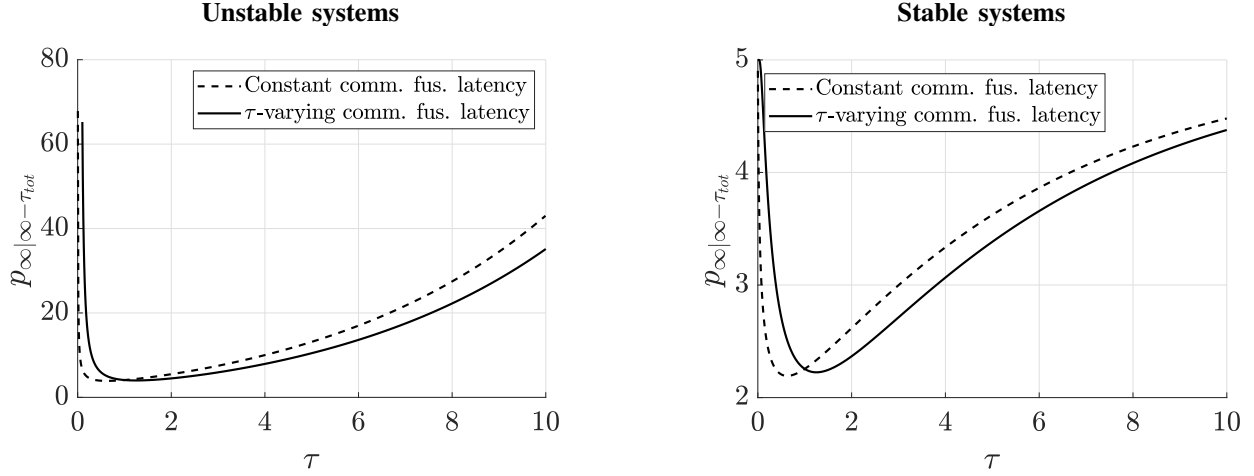


Figure 4: Steady-state error variance  $p_{\infty|\infty-\tau_{tot}}(\tau)$  with  $\sigma_w^2 = \tilde{b} = 1$ ,  $a = 0.1$  (left) and  $a = -0.1$  (right). Dashed line: constant communication delay ((9) with  $\tau_c + \tau_{f,tot} = 1$ ). Solid line:  $\tau$ -varying communication delay ((10) with  $c + fN = 1$ .) Notice that the latter performs better as data get compressed enough (here, for  $\tau > 1$ ).

when the system (5) describes a Brownian motion

$$dx_t = dw_t \quad (13)$$

since the optimal delay has a simple expression.

**Corollary 1** (Brownian motion). *Given system (13) and hypotheses as per Theorem 1, the steady-state error variance  $p_{\infty|\infty-\tau}(\tau)$  has the following expression:*

$$p_{\infty|\infty-\tau}(\tau) = \underbrace{\sqrt{\frac{\tilde{b}\sigma_w^2}{\tau}}}_{f(\tau)} + \underbrace{\sigma_w^2 \tau}_{q(\tau)}$$

admitting the unique global minimum

$$\tau_{opt}^B = \sqrt[3]{\frac{\tilde{b}}{4\sigma_w^2}} \quad (14)$$

Notice that the cubic root in (14) strongly reduces  $\tau_{opt}^B$  sensitivity to system parameters, which may be useful with model uncertainty. Also, the contribution  $f(\tau)$  decreases with the square root of  $\tau$ , while  $q(\tau)$  grows linearly.

#### A. Parameter dependence of optimal delay with constant latency

From the proof of Thm. 1, it turns out that, with constant delays  $\tau_c$  and  $\tau_f$ ,  $\tau_{opt}$  satisfies the following equation:

$$s\tau_{opt}^3 = -a^2\tau_{opt}^2 + \frac{1}{4} \quad s \doteq \frac{\sigma_w^2}{\tilde{b}} \quad (15)$$

We discuss how  $\tau_{opt}$  behaves as a function of each system's parameter according to (15). Notice that  $\sigma_w^2$  and  $\tilde{b}$  do not affect  $\tau_{opt}$  independently, and their effect is gathered in the abstract parameter  $s$ .

**Proposition 1.**  $\tau_{opt}$  is strictly decreasing with  $s$  and  $a^2$ .

*Proof.* See Appendix B.  $\square$

On one hand, Proposition 1 states that it is more convenient to choose small preprocessing delays for “unpredictable systems”, characterized by fast dynamics or large process noise. On the other hand, if the sensor noise is large, it is convenient to perform further preprocessing, which explains why  $\tau_{opt}$  grows with  $b$ . Furthermore,  $\tau_{opt}$  decreases with the number of sensor: the more information is provided, the less time is needed to get an accurate preprocessing. Besides, Proposition 1 yields the following upper bound, which may turn useful with uncertain models.

**Corollary 2.** (Upper bound for  $\tau_{opt}$ )

$$\tau_{opt} \leq \tau_u(|a|, s) := \begin{cases} \frac{1}{2|a|}, & |a| > \sqrt[3]{\frac{s}{2}} \\ \sqrt[3]{\frac{1}{4s}}, & \text{otherwise} \end{cases} \quad (16)$$

Notice that the only case in which equality holds is within Brownian systems, as per Equation 14. Fig. 5 shows the typical behaviour of  $\tau_{opt}$  with respect to the system parameters, together with bound (16).

#### B. Homogeneous network: performance vs sensor amount

If  $p_{\infty|\infty-\tau_{tot}}$  is seen as a function of the number of sensors  $S$  with fixed  $\tau$ ,  $S \in \{1, \dots, N\}$  one may notice that  $p_{\infty|\infty-\tau_{tot}}(S)$  resembles a sampled version of  $p_{\infty|\infty-\tau_{tot}}(\tau)$  in the case with constant  $\tau_c, \tau_f$ . Therefore, there is an *optimal sensor amount*  $S_{opt} \leq N$  minimizing the error variance<sup>2</sup>. Fig. 6 shows performance versus sensor amount: notice that not considering fusion delays may cause poor estimation performance (about 12% less than optimum with  $S_{opt} = 4$  sensors and 32% with  $N$ ).

Such simple analysis motivates formally the sensor selection addressed in Problem 1, where, due to heterogeneity of the

<sup>2</sup>Due to its discrete domain,  $p_{\infty|\infty-h_{tot}}(S)$  may have two points of global minimum with  $p_{\infty|\infty-h_{tot}}(S^*) = p_{\infty|\infty-h_{tot}}(S^* + 1)$ .

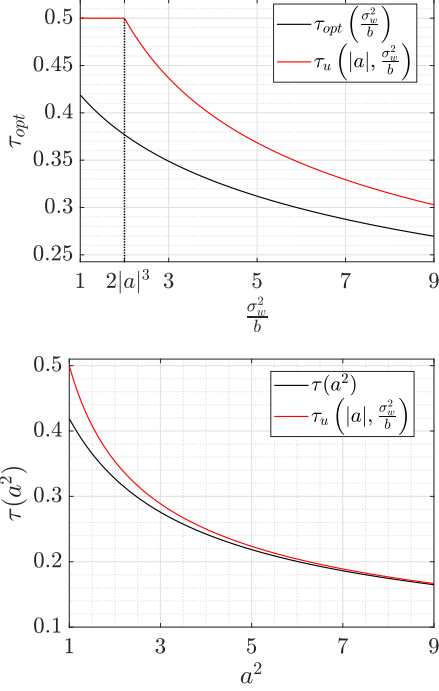


Figure 5: Optimal delay  $\tau_{opt}$  as a function of  $s = \sigma_w^2/\bar{b}$  (with  $a^2 = 1$ , up) and of  $a^2$  (with  $s = 1$  bottom).

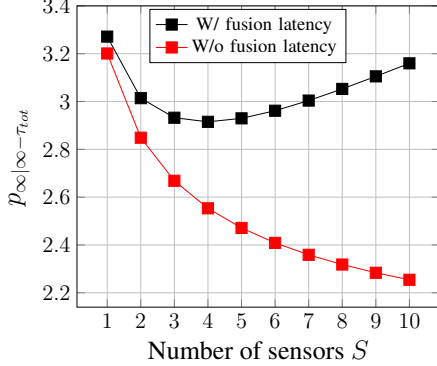


Figure 6: Variance  $p_{\infty|\infty-\tau_{tot}}(S)$  with  $a = -1$ ,  $\sigma_w^2 = 10$ ,  $\bar{b} = h = 0.1$ ,  $h_c = 0.1$ ,  $h_f = 0.02$  (black) and  $h_f = 0$  (red).

network, not only the optimal sensor amount  $S$ , but the very subset  $S \subseteq \mathcal{N}$  must be chosen properly.

#### IV. HOMOGENEOUS NETWORK: GENERAL CASE

In Section III we presented an analytically tractable, simplified situation, which is useful to gather intuition. We now start to considering the more general framework, with homogeneous networks monitoring multidimensional, continuous-time (Subsection IV-A and/or discrete-time systems (Subsection IV-B)).

##### A. Continuous-time multidimensional homogeneous network

We now address the multivariate system (1) with homogeneous sensors (6). In general, explicit solutions for the steady-state measurement-based Kalman filter error variance  $P_{\infty}(\tau)$

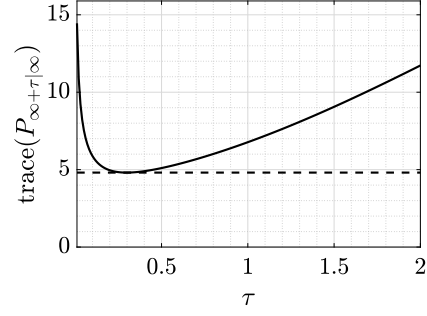


Figure 7:  $\sigma(A) = \{-1, -0.1\}$ ,  $\sigma_w^2 = 10$ .

cannot be written. Therefore, we compute the prediction error variance as

$$P_{\infty|\infty-\tau_{tot}}(\tau) = e^{A\tau} P_{\infty}(\tau) e^{A^T\tau} + Q(\tau) \quad (17)$$

where  $P_{\infty}(\tau)$  is found numerically and

$$Q(\tau) := \int_0^\tau e^{As} Q e^{A^T s} ds \quad (18)$$

is the variance of the process noise integral in  $[0, \tau]$ .

1) *Numerical simulations:* To verify if such multivariate framework is consistent with the scalar analysis, we performed numerical simulations with  $n = 2$  and  $Nm = 100$ . The model was put in controllable form with three options for  $\sigma(A)$ . In particular,  $A$ 's eigenvalues were chosen:

- both asymptotically stable, namely  $\Re(\lambda_i(A)) < 0$ ,  $i = 1, 2$ ;
- one asymptotically stable and one simply stable, namely  $\Re(\lambda_1(A)) < 0$ ,  $\Re(\lambda_2(A)) = 0$ ;
- one asymptotically stable and one unstable, namely  $\Re(\lambda_1(A)) < 0$ ,  $\Re(\lambda_2(A)) > 0$ .

Sensors were simulated with a random  $\tilde{C}$ , while  $v_t$  was assigned variance  $I_N \times R(\tau) = I_{100}^{1/\tau}$ .

Fig. 7 shows the typical behaviour of  $\text{trace}(P_{\infty|\infty-\tau_{tot}}(\tau))$ , which turns out to be analogous for both asymptotically stable, simply stable and unstable systems. Consistency with scalar analysis is evident. Also, it can be seen that the sensitivity of  $\tau_{opt}$  with respect to the system noises has the same behaviour studied previously, *i.e.*, it increases with sensor noise and decreases with process noise.

##### B. Discrete-time homogeneous network

We now approach discrete-time models, and start with the discrete counterpart of the homogeneous network (1)–(6):

$$\begin{cases} x_{k+1} = Ax_k + w_k \\ z_k(h) = (I_N \otimes \tilde{C})x_k + v_k(h) \end{cases} \quad (19)$$

where  $w_k \sim (0, Q)$ ,  $h = \lceil \tau/T_s \rceil$  is the discrete preprocessing delay (and similarly for the other delays) and  $v_k(h) \sim (0, I_N \otimes R(h))$ . Notice that, although the names are the same for sake of readability,  $A$ ,  $Q$  and  $R(\cdot)$  do not correspond to the continuous-time model. Consistently with previous notation, we name  $h_c(h)$  and  $h_f(h)$  communication and fusion delays for each sensor, respectively, with  $h_{tot}$  corresponding to (8). With scalar systems ( $A \in \mathbb{R}$ ), the steady-state error variance

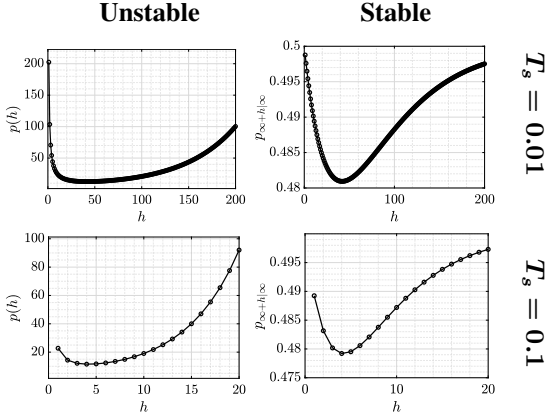


Figure 8: Variance  $p_{\infty|\infty-h_{tot}}(h)$  of discretized systems with continuous-time poles  $a = 1$  (left) and  $a = -1$  (right). The optimal preprocessing delay  $h_{opt}$  may change according to  $T_s$ .

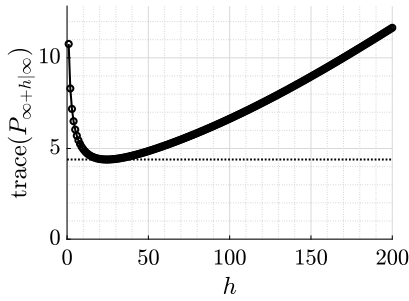


Figure 9: Variance  $p_{\infty|\infty-h_{tot}}(h)$  of discretized system with continuous-time poles  $\sigma(A) = \{-1, -0.1\}$  and process noise variance  $\sigma_w^2 = 10$  (sampling time  $T_s = 0.01$ ).

$p_{\infty|\infty-h_{tot}}(h)$  can be computed in closed form, and it turns out that its curve approximates  $p_{\infty|\infty-\tau_{tot}}(\tau)$  and approaches it as  $T_s$  decreases, as Fig. 8 shows. In particular, an optimal delay  $h_{opt}$  (or two, according to the function values) exists, which minimizes  $p_{\infty|\infty-h_{tot}}(h)$ . Notice that changing  $T_s$  may affect the value of  $h_{opt}$  according to finer/coarser sampling rates.

As for multidimensional systems, numerical simulations confirm the behaviour observed in Subsection IV-A (see Fig. 9). In conclusion, as regards homogeneous networks, both discrete- and continuous-time, multidimensional systems seem consistent with the (feasible) rigorous analysis in continuous-time, scalar case. Such results motivate us to studying the more general heterogeneous-network framework, where we expect to find similar patterns as well as the possibility of optimizing sensor preprocessing.

## V. HETEROGENEOUS NETWORKS

We now address the general problem formulation 3, but stick to the more realistic discrete-time set-up. The available sensor set is  $\mathcal{N} := \{1, \dots, N\}$ , out of which some sensors  $\mathcal{S} \subseteq \mathcal{N}$  need be picked, whose preprocessing delays are gathered in the set  $\mathcal{H} := \{h_i\}_{i \in \mathcal{S}}$ . Each sensor also comes with communication and fusion delays  $h_{c,i}(h_i)$  and  $h_{f,i}(h_i)$ , respectively, and the total fusion delay is  $h_f = \sum_{i \in \mathcal{S}} h_{f,i}(h_i)$ . To lighten notation, the former will be addressed as  $h_{c,i}$  and  $h_{f,i}$  throughout the following sections.

Problem 1 cannot be solved analytically, due to its combinatorial nature. Also, in general the cost function  $P_{\infty|\infty-h_{tot}}(\mathcal{H})$  cannot be computed in closed form, since it is derived from the Riccati equation of Kalman filter. Moreover, given a fixed sensor subset, the cost function changes according to how the sensor delays are sorted, so that even optimizing such simplified setting would imply a comparison between several optima - this fact will be made mathematically precise in the following section. Indeed, with heterogeneous networks we must assume all optimal preprocessing delays  $h_{i,opt}$  be different. That given, a reasonable attempt is resorting to greedy selection algorithms. This section is organized as follows.: in Subsection V-A a model for the heterogeneous network is presented, which is then exploited in Subsection V-B to compute explicitly the cost function  $P_{\infty|\infty-h_{tot}}(\mathcal{H})$ . In Section VI we present the selection algorithms.

### A. Sensor modeling for heterogeneous network

The general set-up presentation in Section II models the network as a single measuring system, encoded by (2). Dealing with a network composed by several sensors, we now aim to dig into such model so as to isolate, when necessary, each sensor as a single subsystem.

In the following, we assume that the sensor subset  $\mathcal{S}$  be fixed, with  $|\mathcal{S}| = S$ . Assuming independent sensors, model (2) is characterized with sensor matrices

$$C = \begin{bmatrix} C_1 \\ \vdots \\ C_S \end{bmatrix} \quad R(\mathcal{H}) = \begin{bmatrix} R_1(h_1) & & \\ & \ddots & \\ & & R_S(h_S) \end{bmatrix} \quad (20)$$

with variance  $R_i(\cdot)$  as per (7) with (suitably rescaled) coefficient  $b_i$  and, without loss of generality, active sensors sorted according to their total preprocessing-and-communication delay (*sensor delay*), namely  $h_1 + h_{c,1} \leq \dots \leq h_S + h_{c,S}$  (with both constant and  $h$ -varying communication and fusion latency). Such choice is convenient for the cost function computation.

*Remark 3.* Although the selected sensors in  $\mathcal{S}$  are labelled with 1, 2, etc., such labels do *not* correspond to the original ones in the available set  $\mathcal{N}$ ! Such relabelling only avoids a too heavy notation.

### B. Cost function computation

Our aim is providing an iterative algorithm to compute exactly the cost function  $P_{\infty|\infty-h_{tot}}(\mathcal{H})$ , which will be exploited by the designed greedy algorithms to assess the goodness in choosing certain sensors. Notice that here Assumption 1 is crucial in simplifying computations.

At each time step  $k$ , all available information at fusion centre is (c.f. Section II)  $\mathcal{Z}_k(\mathcal{H})$ , storing all received delayed data. Let us define

$$\hat{x}_{k-h|k-h-1}^k(\mathcal{H}) \doteq \hat{\mathbb{E}}[x_{k-h} | \{z_\ell \in \mathcal{Z}_k(\mathcal{H}) : \ell \leq k-h\}]$$

$$P_{k-h|k-h-1}^k(\mathcal{H}) \doteq \text{var}(\hat{x}_{k-h|k-h-1}^k)$$

namely,  $P_{k-h|k-h-1}^k(\mathcal{H})$  is the error variance associated with the one-step-ahead prediction  $\hat{x}_{k-h|k-h-1}(\mathcal{H})$  computed with

the available information at time  $k$ . In particular, as soon as  $k - h - 1$  gets bigger than the last received data (equivalently,  $h - 1$  is smaller than the smallest sensor-and-communication delay), the estimation has to be computed via open-loop steps only. We are interested in computing  $P_{k|k-1}^k$ , *i.e.*, the error variance at current time with currently available information. Throughout the rest of this section, for sake of readability, we address each sensor delay  $h_i + h_{c,i}$  as  $\tilde{h}_i$ . Since by time  $k$  all sensors provided the data they collected at time  $k - \tilde{h}_S$  - corresponding to the freshest measurement sent by the most-delayed sensor -, the first passage involves an update with measurements of the prediction  $\hat{x}_{k-\tilde{h}_S+1|k-\tilde{h}_S}^{k-1}(\mathcal{H})$  of  $x_{k-\tilde{h}_S}$  computed at the previous time step. Such update is nothing but the one-step-ahead Kalman prediction with all sensor data: therefore, the variance  $P_{k-\tilde{h}_S+1|k-\tilde{h}_S}^k(\mathcal{H})$  attains the steady-state value  $P_\infty(\mathcal{H})$  satisfying the ARE

$$P_\infty(\mathcal{H}) = A \left( (P_\infty(\mathcal{H}))^{-1} + \Gamma(\mathcal{H}) \right)^{-1} A^T + Q$$

where

$$\Gamma(\mathcal{H}) \doteq C^T (R(\mathcal{H}))^{-1} C = \sum_{i \in \mathcal{S}} C_i^T (R_i(h_i))^{-1} C_i$$

is the information matrix associated with all measurements. The ARE measurement-update is computed with Kalman filter in information form: this allows for handling more easily the sensor fusion, whose action is embedded in  $\Gamma(\mathcal{H})$ , and also is useful when some sensors has infinite variance at some state location<sup>3</sup>. Notice that having independent sensors yields a nice expression for this matrix, where each sensor's contribution is visible and disjoint from the others.

After  $k - \tilde{h}_S + 1$ , only some measurements have been received. Dealing with such a partial information is equivalent to considering a time-varying sensor model, with the state-output matrix becoming sparser and sparser as some sensors gather too much delay, resulting in no transmitted information. Model (2) can be rewritten as follows:

$$z_{k-h}(\mathcal{H}_h) = \tilde{C}_h x_{k-h} + v_{k-h}(\mathcal{H}), \quad 1 \leq h < \tilde{h}_S$$

where

$$\mathcal{H}_h \doteq \{h_i \in \mathcal{H} : \tilde{h}_i \leq h\}$$

are the preprocessing delays of sensors which provided data for  $x_{k-h}$  (having inferior sensor delay  $\tilde{h}_i \leq h$ ),

$$s(h) = \arg \max_{i \in \mathcal{S}} \{\tilde{h}_i : \tilde{h}_i \leq h\}$$

is the most-delayed sensor (with largest sensor delay) among those providing data for  $x_{k-h}$ , and

$$\tilde{C}_h = \begin{bmatrix} C_1^T & \dots & C_{s(h)}^T & 0_{n \times m_{s(h)+1}} & \dots & 0_{n \times m_S} \end{bmatrix}^T$$

is the time-varying state-output matrix, with zero rows in correspondence to sensors which have not provided data referring to  $x_{k-h}$  due to their delay  $\tilde{h}_i > h$ .

In words,  $i$ -th sensor provides data referring to instants  $\mathcal{K} = [k - \tilde{h}_S, k - \tilde{h}_i]$ : inside such interval (*i.e.*, when central

estimation exploits data referring to those times), it holds  $\tilde{h}_i \in \mathcal{H}_h$  and its data are available for fusion, because the currently computed estimate  $\hat{x}_{k-h|k-h-1}^k(\mathcal{H})$  refers to an older time that the last measurement provided by  $i$ . Equivalently,  $\hat{x}_{k-h|k-h-1}^k(\mathcal{H})$  has  $k - h - 1 \in \mathcal{K}$ , namely, it has more “delay” than the data provided by  $i$ . As soon as the central station updates the estimate with measurements collected at time  $k - \tilde{h}_i$ ,  $s(\tilde{h}_i) = i$  since the  $i$ -th sensor had sent its freshest datum at that time. From time instant  $k - \tilde{h}_i + 1$ , such sensor (and all more-delayed ones) is considered as if not monitoring the system any more, and its contribution to the overall state-output matrix  $\tilde{C}(\cdot)$  is annihilated.

Within this framework, the general one-step partial-measurement update can be written as follows:

$$\begin{aligned} P_{k-h+1|k-h}^k(\mathcal{H}_h) &= \\ &= A \left( \left( P_{k-h|k-h-1}^k(\mathcal{H}_{h+1}) \right)^{-1} + \Gamma(\mathcal{H}_h) \right)^{-1} A^T + Q \end{aligned}$$

with  $\tilde{h}_1 \leq h < \tilde{h}_S$ , initial condition  $P_{k-\tilde{h}_S+1|k-\tilde{h}_S}^k(\mathcal{H}_{\tilde{h}_S}) = P_\infty(\mathcal{H})$ , and time-varying information matrix

$$\Gamma(\mathcal{H}_h) = \sum_{i \leq s(h)} \tilde{C}_i^T (R_i(h_i))^{-1} \tilde{C}_i$$

Notice that the same set of sensors may provide data for consecutive time instants, in general. To compact, let us define the following functions associated with time-varying Kalman filter:

open-loop time update:

$$\mathcal{T}(P) \doteq A P A^T + Q$$

measurement update with data collected at  $k - h$  (delay  $h$ ):

$$\mathcal{M}(P, \mathcal{H}_h) \doteq (P^{-1} + \Gamma(\mathcal{H}_h))^{-1}$$

one-step prediction with data collected at  $k - h$ :

$$\mathcal{U}(P, \mathcal{H}_h) \doteq \mathcal{T} \circ \mathcal{M}(P, \mathcal{H}_h)$$

multi-step prediction with data collected between  $k - h_i + 1$  and  $k - h_j$  (included):

$$\mathcal{U}^{h_i-h_j}(P, \mathcal{H}_{h_{i-1}}) \doteq \mathcal{U}(\dots \mathcal{U}(P, \mathcal{H}_{h_{i-1}}), \dots, \mathcal{H}_{h_j})$$

Notice that if  $h_i = h_j$ ,  $\mathcal{U}^{h_i-h_j}(\cdot, \cdot)$  leaves  $P$  unchanged, while if  $h_i = h_j + 1$  there is only one sample to be considered, and  $\mathcal{U}^{h_i-h_j}(\cdot, \mathcal{H}_{h_{i-1}})$  boils down to  $\mathcal{U}(\cdot, \mathcal{H}_{h_j})$ .

Then, we can write compactly the overall measurement update with all available information at time  $k$ ,  $\mathcal{Z}_k(\mathcal{H})$ , starting from the previous estimate computed with all sensor data:

$$\begin{aligned} P_{k-\tilde{h}_1+1|k-\tilde{h}_1}^k(\mathcal{H}) &= \mathcal{U}^{\tilde{h}_S-\tilde{h}_1}(P_\infty(\mathcal{H}), \mathcal{H}_{\tilde{h}_S-1}) = \\ &= \mathcal{U}^{\tilde{h}_2-\tilde{h}_1} \left( \dots \mathcal{U}^{\tilde{h}_S-\tilde{h}_{S-1}}(P_\infty(\mathcal{H}), \mathcal{H}_{\tilde{h}_S-1}), \dots, \mathcal{H}_{\tilde{h}_1} \right) \end{aligned} \quad (21)$$

where each multi-hop update  $\mathcal{U}^{\tilde{h}_i-\tilde{h}_{i-1}}$  involves the sensor subset  $\mathcal{S}_i = \{1, \dots, i - 1\}$ .

At the first updating, all sensor data are available and therefore the error variance attains the steady-state value  $P_\infty(\mathcal{H})$ . After the oldest measurements (collected at time  $k - \tilde{h}_S$ ) are used,

<sup>3</sup>Such situation may occur if a sensor lacks full state observability or is forced to output data after a minimum runtime.

sensor  $S$  is useless, since it provided no data collected after  $k - \tilde{h}_S$  yet - i.e.,  $\tilde{C}_h$  is zero in correspondence to the rows of  $S$ , for  $h < \tilde{h}_S$ .

Then, measurements transmitted by sensors  $\{1, \dots, S-1\}$  and collected in time interval  $\mathcal{K}_{S-1} = [k - \tilde{h}_S + 1, k - \tilde{h}_{S-1}]$  are used. The maximum of  $\mathcal{K}_{S-1}$  corresponds to the latest measurement provided by sensor  $S-1$ , which therefore is “discarded” after processing all measurements collected in  $\mathcal{K}_{S-1}$ : such fusion corresponds to  $\mathcal{U}^{\tilde{h}_S - \tilde{h}_{S-1}}(P_\infty(\mathcal{H}), \mathcal{H}_{\tilde{h}_{S-1}})$ . The iterations continues until all sensor data have been exploited. The final steps for computing  $\tilde{x}_{k|k-1}^k$  are pure open-loop predictions, as no more data are available. Such prediction compensates for both the least-delayed sensor delay and the total fusion delay induced by all sensors:

$$P_{k|k-1}^k(\mathcal{H}) = \mathcal{T}^{\tilde{h}_1 - 1 + h_f} \left( P_{k - \tilde{h}_1 + 1 | k - \tilde{h}_1}^k(\mathcal{H}) \right) \quad (22)$$

where

$$\mathcal{T}^h(P) = \underbrace{\mathcal{T} \circ \dots \circ \mathcal{T}}_{h \text{ times}}(P), \quad \mathcal{T}^0(P) \doteq P$$

is the (possibly) multi-step time update.

## VI. GREEDY ALGORITHMS FOR SENSOR SELECTION

Since minimizing (22) jointly with respect to sensor subset  $S$  and computational delays  $\mathcal{H}$  is hard, the followed approach was twofold. On one hand, the selection task was devoted to algorithms selecting the most performing subset, by greedily adding or removing one sensor at a time until a sub-optimal performance is hit. On the other hand, each tentative subset’s performance is assessed by a subroutine aiming to find near-optimal preprocessing delays for that subset. The following section illustrates how such a subroutine works, while Subsection VI-B present the greedy selection algorithms. The latter only deal with constant-latency models: their extension to the  $h$ -varying case (which is possibly quite straightforward) is objective of future work.

### A. Near-optimal delay selection

In general, a closed-form solution for Kalman recursion equilibrium cannot be computed, therefore the cost function (i.e., variance (22)) has to be computed numerically. That

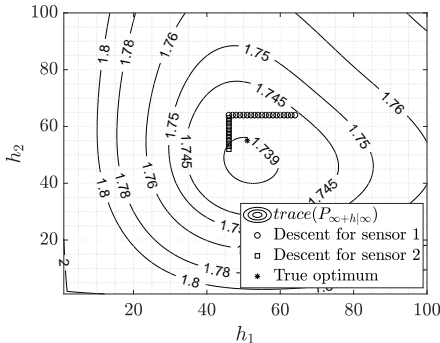


Figure 10: Level curves of  $\text{trace}(P_{\infty|h|(\infty)})$  with constant latency  $h_{c,i}$ ,  $h_{f,i}$ . Component-wise descent is also visible.

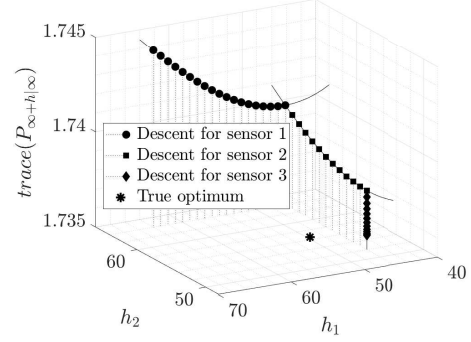


Figure 11: Component-wise descent with three sensors.

given, a greedy approach was also chosen for this optimization task. The intuition gathered from studying homogeneous networks suggests that the variance should be convex or quasi-convex also with heterogeneous sensors/delays. Consistency of this hypothesis has been assessed by numerical simulations. Fig. 10 shows the cost function level curves for a three-sensor network, with one delay fixed: (strict) quasi-convexity appears to hold also within such scenario.

Inspired by intuition and simulations, we designed a *component-wise descent*: one sensor’s delay at a time is optimized, starting from an initial point and “sliding” down to the minimum of its associated one-dimensional profile, with all other delays fixed. The subroutine steps for this example are shown in Fig. 10–Fig. 11, together with the true optimum. Algorithm 1 shows the subroutine steps. After initialization, the external loop (lines 3–??) performs the optimization with respect to one sensor  $i$  at a time (one-dimensional minimization), making only delay  $h_i$  vary (line 6) with the other  $h_j, j \neq i$  fixed, and computing the corresponding performance  $P_{curr}$  (line 7) until this is not better than the already-achieved one  $P_{min}$  (line 8). The ever-decreasing delay update in line 6 is motivated by assuming the initial delays  $\mathcal{H}_I$  be always greater than the optimal ones. Given the function structure, such assumptions could be satisfied, e.g., by setting each initial point to the maximum allowed delay. In the following section, we present a trick to initialize the subroutine smartly.

---

#### Algorithm 1 compWiseDescent subroutine

---

**Require:** System  $(A, Q)$ , sensor set  $\mathcal{S}$  with state-output  $C_i$ , noise variance  $R_i(\cdot)$ , communication and fusion delays  $h_{c,i}$ ,  $h_{f,i}$  for each sensor  $i \in \mathcal{S}$ , initial delays  $\mathcal{H}_I$ .

**Ensure:** Sub-optimal delays  $\mathcal{H}^*$ , variance  $P_{k|k-1}^k(\mathcal{H}^*)$ .

- 1:  $P_{curr} \leftarrow$  compute  $P_{k|k-1}^k(\mathcal{H}_I)$  as per (22);
  - 2:  $\mathcal{H}, \mathcal{H}^* \leftarrow \mathcal{H}_I$ ;
  - 3: **for each**  $i \in \mathcal{S}$  **do**
  - 4:   **repeat**
  - 5:      $P_{min} \leftarrow P_{curr}$ ;
  - 6:      $\mathcal{H}[i] \leftarrow \mathcal{H}[i] - 1$
  - 7:      $P_{curr} \leftarrow$  compute  $P_{k|k-1}^k(\mathcal{H})$  as per (22);
  - 8:     **until**  $\text{trace}(P_{min}) \leq \text{trace}(P_{curr})$
  - 9:      $\mathcal{H}^*[i] \leftarrow \mathcal{H}[i] + 1$ ;
  - 10: **end for**
-

## B. Near-optimal sensor selection

1) *Additive selection*: The first strategy consists in a greedy algorithm which tries to improve performance by continuously adding one sensor at a time, until the minimum achievable steady-state prediction error variance is found.

Algorithm 2 shows the workflow of such a procedure. First of all, single-sensor optimal performances are computed for all available sensors (line 2): namely, each sensor is taken alone and the performance is optimized on a single-sensor network. Notice that, by construction, the descent subroutine outputs the true optima in this case, in virtue of initialization with the maximum allowed delay  $h_M$  (c.f. Fig. 9, which is equivalent to a single-sensor network up to suitable parameters rescaling). The best-performing sensor is used to initialize the best variance  $P_{min}$ , optimal sensor subset  $\mathcal{S}^*$  and delay set  $\mathcal{H}^*$  (lines 4–5). Then, at each iteration the external loop seeks a new sensor to add to the current best subset, and stops when no additive sensor manages to improve the overall performance (or when all sensors have been added, lines 6–24). The inner loop (lines 9–19), given the current-best subset  $\mathcal{S}^*$ , enlarges it with any sensor *toTry* not already included, trying one at a time, getting the tentative subset  $\mathcal{S}_{curr}$  (lines 10) and computing its near-optimal performance with the `compWiseDescent` subroutine (lines 11–13). As soon as such tentative subset manages to outperform the current best, sensor *toTry* is labelled as the one *toAdd* and the best achieved performance is updated accordingly (lines 14–18). Notice that the temporary variable  $\mathcal{H}_{curr}^*$  is needed to store the best performance of tentative subsets  $\mathcal{S}_{curr}$  without losing  $\mathcal{H}^*$ , which is used to initialize the descent in line 11. Finally, the external loop checks if any new subset outperformed the current best: if this is the case, sensor *toAdd* joins definitely  $\mathcal{S}^*$ , and the optimal delay set  $\mathcal{H}^*$  is updated, as well (lines 20–23).

We now take a deeper insight on descent initialization (line 11). This exploits the analytical result provided by Proposition 1: in particular, the latter states that the optimal delay  $\tau_{opt}$  is strictly decreasing with the number of sensors  $S$ , within continuous-time homogeneous networks. Such property has been assessed with heterogeneous sensors, as well, by means of simulations, one out of whom is showed in Table I. As the set gets larger, all optimal delays decrease: for instance, the first sensor's is 80 with single-node performance, then drops to 57 when the second sensor is added and further decreases to 51 with the full three-sensor set. Such intuition allows for the smart descent initialization as per line 11: as the subset  $\mathcal{S}^*$  is enlarged, *i.e.*, a tentative sensor  $i$  is added, all optimal delays can only decrease. Therefore, the initial condition for component-wise descent is set equal to the delays  $\mathcal{H}^*$  and  $h_i^s$  achieved so far for sensors in  $\mathcal{S}_{curr}$ , saving iterations with respect to initializing the delays “dummy”, *e.g.*, by setting each initial condition equal to the maximal allowed delay  $h_M$ . We may formalize such empirical intuition as follows:

$$h_{i,opt} \leq h'_{i,opt} \quad \forall \mathcal{S}' \subseteq \mathcal{S}, i \in \mathcal{S}', h_{i,opt} \in \mathcal{H}^*, h'_{i,opt} \in \mathcal{H}'^*$$

where  $h_{i,opt}$  corresponds to the optimal performance achieved by  $\mathcal{S}$ , and similarly for  $h'_{i,opt}$ , with any subset  $\mathcal{S}' \subseteq \mathcal{S}$  contain-

One sensor	Two sensors	Three sensors
Sensor 1: 80	Sensor 1: 57 Sensor 2: 58	Sensor 1: 51 Sensor 2: 55 Sensor 3: 50
Sensor 2: 64	Sensor 1: 64 Sensor 3: 62	
Sensor 3: 76	Sensor 2: 58 Sensor 3: 55	

Table I: Optimal delays with one, two and three sensors, with a stable, heterogeneous network and constant communication and fusion delays.

ing sensor  $i$ . Additive selection works after the main principle that, if  $\mathcal{S}$  is optimal for  $S$  sensors, then any larger subset must contain it to provide an equal or better performance. This may not be the case, and our specific framework appears to be even more varied by different fusion delays, so that a well-performing set may become inadequate when a new sensor is added because of too large fusion latency.

### Algorithm 2 Additive sensor selection

**Require:** System  $(A, Q)$ , available sensor set  $\mathcal{N}$  with state-output  $C_i$ , noise variance  $R_i(\cdot)$ , communication and fusion delays  $h_{c,i}$ ,  $h_{f,i}$  for each sensor  $i \in \mathcal{N}$ , maximal allowed delay  $h_M$ .

**Ensure:** Sub-optimal sensor set  $\mathcal{S}^*$ , delay set  $\mathcal{H}^*$ .

```

1: for each  $i \in \mathcal{N}$  do
2:    $[h_i^s, P_i^s] \leftarrow \text{compWiseDescent}\{A, Q, \{i\}, h_M\}$ ;
3: end for
4:  $\text{bestSingle} \leftarrow \arg \min_{i \in \mathcal{N}} P_i^s$ ;  $P_{curr} \leftarrow P_{\text{bestSingle}}^s$ ;
5:  $\mathcal{S}^* \leftarrow \{\text{bestSingle}\}$ ;  $\mathcal{H}^* \leftarrow \{h_{\text{bestSingle}}^s\}$ ;
6: repeat
7:    $P_{min} \leftarrow P_{curr}$ ;
8:    $\text{toAdd} \leftarrow \text{none}$ ;
9:   for each  $\text{toTry} \in \mathcal{N} \setminus \mathcal{S}^*$  do
10:     $\mathcal{S}_{curr} \leftarrow \mathcal{S}^* \cup \{\text{toTry}\}$ ;
11:     $\mathcal{H}_I \leftarrow \mathcal{H}^* \cup \{h_{\text{toTry}}^s\}$ ;
12:     $[\mathcal{H}_{curr}, P_{curr}] \leftarrow$ 
13:       $\text{compWiseDescent}\{A, Q, \mathcal{S}_{curr}, \mathcal{H}_I\}$ ;
14:    if  $\text{trace}(P_{min}) > \text{trace}(P_{curr})$  then
15:       $P_{min} \leftarrow P_{curr}$ ;
16:       $\mathcal{H}_{curr}^* \leftarrow \mathcal{H}_{curr}$ ;
17:       $\text{toAdd} \leftarrow \text{toTry}$ ;
18:    end if
19:   end for
20:   if  $\exists \text{toAdd}$  then
21:      $\mathcal{S}^* \leftarrow \mathcal{S}^* \cup \{\text{toAdd}\}$ ;
22:      $\mathcal{H}^* \leftarrow \mathcal{H}_{curr}^*$ ;
23:   end if
24: until  $\text{trace}(P_{min}) \leq \text{trace}(P_{curr})$  or  $|\mathcal{S}| = N$ 

```

*Remark 4.* It may happen that single-sensor performances in line 2 cannot be evaluated, which would be the case if some pair  $(A, C_i)$  are not detectable. If only some sensors are “blind”, then initialization would only include detectable single-node subsystems. If no sensor can detect the state, the

algorithm could still work, by replacing single-sensor-based initialization with the greedy selection of a subset providing detectability. Such procedure could simply find the minimum sensor amount  $K$  for which the system is detectable, by assessing detectability of all subsystems  $(A, [C_i^T, \dots, C_k^T]^T)$ ,  $k \leq K$ , and then initialize  $\mathcal{S}^*$  with the best subset of cardinality  $K$ .

2) *Fast additive selection*: This heuristics works with a slightly similar principle to the previous one, but is far more rough and is mostly useful for comparison with the previous algorithm. After having computed all single-sensor optima and initialized near-optimal subset and delays, tentative sensors are added from the most to the least performing (as for single-sensor performance, line 8), until no performance improvement is possible. The external loop between lines 6–17 is analogous to 2, adding a sensor at each iteration (line 8) and computing the new performance (lines 9–12). If the latter has improved, the new set is confirmed (lines 13–16).

This selection works after the dummy principle that the sensors performing best individually also are the best choice when grouped together. This does not take into account that, for example, single-excellent sensors with similar  $C_i$  may perform worse, together, than rougher sensors providing complementary information. In addition, different fusion and communication latency may lead to unexpected performances. In practice, this algorithm may be useful in the following situations: either the sensors are very similar one to each other, providing more or less the same information and fusion delay, or the allowed runtime for the very algorithm is small (*e.g.*, for on-line tasks), so that a quick response is needed.

---

**Algorithm 3** Fast additive sensor selection

---

**Require:** System  $(A, Q)$ , available sensor set  $\mathcal{N}$  with state-output  $C_i$ , noise variance  $R_i(\cdot)$ , communication and fusion delays  $h_{c,i}$ ,  $h_{f,i}$  for each sensor  $i \in \mathcal{N}$ , maximal allowed delay  $h_M$ .

**Ensure:** Sub-optimal sensor set  $\mathcal{S}^*$ , delay set  $\mathcal{H}^*$ .

```

1: for each  $i \in \mathcal{N}$  do
2:    $[h_i^s, P_i^s] \leftarrow \text{compWiseDescent}\{A, Q, \{i\}, h_M\}$ ;
3: end for
4:  $\text{bestSingle} \leftarrow \arg \min_{i \in \mathcal{N}} P_i^s$ ;  $P_{\text{curr}} \leftarrow P_{\text{bestSingle}}^s$ ;
5:  $\mathcal{S}^* \leftarrow \{\text{bestSingle}\}$ ;  $\mathcal{H}^* \leftarrow \{h_{\text{bestSingle}}^s\}$ ;
6: repeat
7:    $P_{\min} \leftarrow P_{\text{curr}}$ ;
8:    $\text{toTry} \leftarrow \arg \min_{i \in \mathcal{N} \setminus \mathcal{S}^*} P_i^s$ ;
9:    $\mathcal{S}_{\text{curr}} \leftarrow \mathcal{S}^* \cup \{\text{toTry}\}$ ;
10:   $\mathcal{H}_I \leftarrow \mathcal{H}^* \cup \{h_{\text{toTry}}^s\}$ ;
11:   $[\mathcal{H}_{\text{curr}}, P_{\text{curr}}] \leftarrow$ 
12:     $\text{compWiseDescent}\{A, Q, \mathcal{S}_{\text{curr}}, \mathcal{H}_I\}$ ;
13:  if  $\text{trace}(P_{\min}) > \text{trace}(P_{\text{curr}})$  then
14:     $\mathcal{S}^* \leftarrow \mathcal{S}^* \cup \{\text{toTry}\}$ ;
15:     $\mathcal{H}^* \leftarrow \mathcal{H}_{\text{curr}}$ ;
16:  end if
17: until  $\text{trace}(P_{\min}) \leq \text{trace}(P_{\text{curr}})$  or  $|\mathcal{S}| = N$ 

```

---

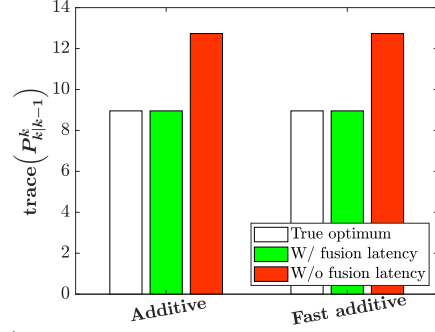


Figure 12: Optimal performance (white bars) and output of the selection algorithms (green and red bars). Green bars: fusion latency is considered ( $h_{f,i} = 20$ ). Red bars: fusion latency is not considered ( $h_f = 0$ ). Notice the performance drop as a consequence of neglecting the latency contribution produced by fusion.

## VII. EXPERIMENTAL RESULTS

In order to assess if the designed algorithm is effective, numerical simulations have been run. The experimental framework features a four-dimensional system, with poles  $\sigma(A) \approx \{1, 0.999, 0.995, 0.99\}$ , driven by a process noise with variance equal to zero at all locations except for  $(Q)_{4,4} \approx 0.0098$ . The available set  $\mathcal{N}$  is composed of six sensors having all sparse  $C_i$  matrices and decreasing noise coefficients  $b_i$ . The maximal allowed delay  $h_M$  to assess individual performances was chosen equal to 100 (all single-performance optima being lower than that). Since brute-force-search complexity is factorial with the total number of sensors and exponential with the delays, the allowed delay range was suitably restricted in order to compute the true optimal sensor subset and preprocessing delays. In particular, 7 total delay options were allowed, ranging from 30 to 60 (included) with step 5. To be consistent, such adjustment was applied also to the descent subroutine, which therefore had line 6 slightly modified, hopping downwards from one allowed delay to the other. The actual presence of all optima inside the restricted interval was cross-checked with the greedy algorithms, to ensure the latter did not outperform the brute-force search.

Fig. 12 shows a comparison between the true optimal performance, *i.e.*, the minimum achievable variance  $P_{k|k-1}^k$ , and how the algorithm output sensors perform with the selected delays. While both the algorithms are able to hit the optimum when fed with all information (*c.f.* white and green bars), neglecting fusion delay may lead to serious performance drops (red bars), which in this situation mean an increased trace of the variance by about 42%.

Such drop is mostly caused by all sensors being selected, while the optimal solution in this case is to pick only two sensors (4 and 5), as 13 shows, limitedly to additive selection. Stars represent the optima within sensor-delay space: while in the first case both the optimal subset and delays are selected, in the second case all sensor are taken, since the absence of fusion latency leads the selection algorithm to include as many sensors as possible to decrease sample variance.

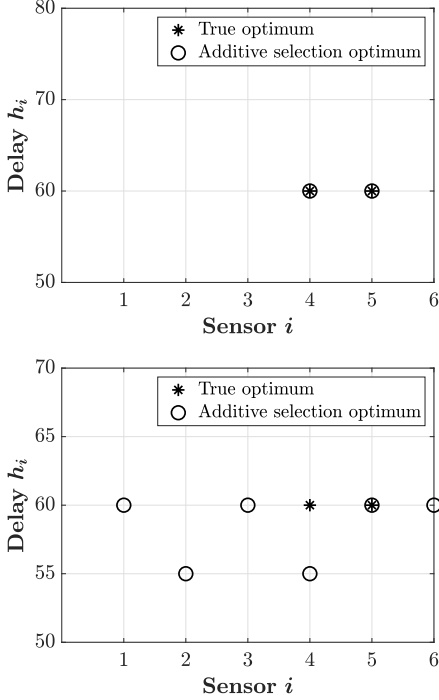


Figure 13: Optimal sensor subset/delays compared to additive selection output. Top box: fusion latency is considered. Bottom box: fusion latency is neglected.

## VIII. CONCLUSIONS AND FUTURE WORKS

In this paper, we investigate optimal estimation in a processing network in the presence of communication and computational delays. We model sensor-side preprocessing as a stochastic measurement model, whose noise intensity decreases with the computational delay. Similarly, communication and fusion latencies are modeled as a constant or decreasing function of computation delay, simulating data compression. For the continuous-time, fixed-homogeneous-network, scalar scenario, we prove that the resulting trade-off between preprocessing and computation can be optimized analytically with respect to the preprocessing delay. Such result also holds for discrete-time systems and has been assessed within multi-dimensional scenarios, which follow the same trend according to numerical simulations. Extending the framework to heterogeneous networks, we broaden the problem as well to optimal sensor selection out of an available sensor set. Due to the combinatorial nature of such problem, and to the general impossibility to computing the cost function in closed form, we develop two greedy algorithm, together with a subroutine for near-optimal delay selection. Numerical experiments performed on a four-dimensional system show the effectiveness of such algorithms, and mostly measure the performance plummet due to neglecting some latency contribution present in the model.

Future works about the proposed approach may be multifold. First of all, the selection algorithms should be extended in order to address also varying communication and fusion latency. Such extension may be quite straightforward is the

cost function shape were similar to the analyzed case. In addition, their performance should analytically studied, in order to endow them with suitable guarantees. An option in this way would involve submodularity and/or complexity analysis. Finally, the employed model could be made arbitrarily complex introducing non-ideal communication, coming with unreliability and packet loss, limited bandwidth and channel capacity, and random latency. Preprocessing latency may be randomized as well, accounting for more realistic sensor models.

## APPENDIX A PROOF OF THEOREM 1

The steady-state Kalman error variance of the outdated, measurement-based estimate  $\hat{x}_{t-\tau_{tot}}(\tau)$  can be computed as the unique equilibrium of the continuous-time ARE associated with the filter, and it reads

$$p_{\infty}(\tau) = \frac{\tilde{b}}{\tau} \left( a + \sqrt{a^2 + \frac{\sigma_w^2}{\tilde{b}} \tau} \right) \quad (23)$$

where the total information matrix is, according to (6) and (7)

$$(\mathbb{1}_N \times \tilde{C})^T [R(\tau)]^{-1} (\mathbb{1}_N \times \tilde{C}) = N \gamma \frac{\tau}{b}$$

In order to compensate for the total delay, a model-based open-loop prediction has to be performed, covering a time interval with length  $\tau_{tot}$ . Such prediction yields the current-time estimate  $\hat{x}_t(\tau)$ , computed with partially outdated measurements. The error associated with such prediction has dynamics

$$d\tilde{x}_s(\tau) = a\tilde{x}_s(\tau)ds + dw_s, \quad t - \tau_{tot} \leq s \leq t \quad (24)$$

Then, the final error is given by solving (24) as a Cauchy problem with initial condition  $\tilde{x}_{t-\tau_{tot}}(\tau)$ :

$$\tilde{x}_t(\tau) = e^{a\tau_{tot}} \tilde{x}_{t-\tau_{tot}}(\tau) + \bar{w}(\tau_{tot})$$

where  $\bar{w}(\tau_{tot})$  is the stochastic integral of  $w_s$  in the interval  $[t - \tau_{tot}, t]$ . The steady-state prediction error variance is then

$$\begin{aligned} p_{\infty|\infty-\tau_{tot}}(\tau) &\stackrel{(i)}{=} \text{var}(e^{a\tau_{tot}} \tilde{x}_{t-\tau_{tot}}(\tau)) + \text{var}(\bar{w}(\tau_{tot})) = \\ &= e^{2a\tau_{tot}} p_{\infty}(\tau) + \frac{\sigma_w^2}{2a} (e^{2a\tau_{tot}} - 1) \end{aligned}$$

where (i) is motivated by uncorrelated terms. Indeed,  $\tilde{x}_{t-\tau_{tot}} \in \text{span}\{x_{t_0}, w_s, v_s : t_0 \leq s \leq t - \tau_{tot}\}$ , while  $\bar{w}(\tau_{tot}) \in \text{span}\{w_s : t - \tau_{tot} \leq s \leq t\}$ . The only sample providing nonzero correlation is  $w_{t-\tau_{tot}}$ , but having zero Lebesgue measure its contribution is null.

Variance  $p_{\infty|\infty-\tau_{tot}}(\tau)$  is strict quasi-convex with both constant and  $\tau$ -varying communication and fusion delays. Such property can be proved, e.g., with a graphical analysis, checking strict convexity of its sublevel sets. In virtue of both this fact and limits (12), we conclude that the point of minimum exists unique and is different from zero, i.e., strictly positive. In particular, with constant delays  $\tau_c, \tau_f$ , it can be seen (by studying the derivative  $p'_{\infty|\infty-\tau_{tot}}(\tau)$ ) that the optimal preprocessing delay  $\tau_{opt}$  satisfy the following equation:

$$\frac{\sigma_w^2}{b} \tau_{opt}^3 = -a^2 \tau_{opt}^2 + \frac{1}{4} \quad (25)$$

## APPENDIX B

### PROOF OF PROPOSITION 1

For this proof we are going to exploit the implicit function theorem, whose statement is recalled for convenience.

**Theorem 2** (Dini's theorem). *Let  $F$  be a continuously differentiable function on some open  $D \subset \mathbb{R}^2$ . Assume that there exists a point  $(\bar{x}, \bar{y}) \in D$  such that:*

- $F(\bar{x}, \bar{y}) = 0$ ;
- $\frac{\partial F}{\partial y}(\bar{x}, \bar{y}) \neq 0$ .

*Then, there exist two positive constant  $a, b$  and a function  $f : I_{\bar{x}} := (\bar{x} - a, \bar{x} + a) \mapsto J_{\bar{y}} := (\bar{y} - b, \bar{y} + b)$  such that*

$$F(x, y) = 0 \iff y = f(x) \quad \forall x \in I_{\bar{x}}, \forall y \in J_{\bar{y}}$$

*Moreover,  $f \in C^1(I_{\bar{x}})$  and*

$$f'(x) = -\frac{F_x(x, f(x))}{F_y(x, f(x))} \quad \forall x \in I_{\bar{x}}$$

We can see the left-hand term in eq. (15) as a one-parameter function of two positive-valued variables, namely

$$F : \mathbb{R}_+ \times \mathbb{R}_+ \rightarrow \mathbb{R}, (\pi, \tau) \mapsto F(\pi, \tau) = s\tau^3 + a^2\tau^2 - \frac{1}{4}$$

with  $\pi = \{s, a^2\}$ . First of all, let us check if Dini's theorem hypotheses are satisfied: given a solution  $(\bar{\pi}, \bar{\tau}_{opt})$  of eq. (15) it holds

- $F(\bar{\pi}, \bar{\tau}_{opt}) = 0$ , by construction;
- $F_{\tau}(\bar{\pi}, \bar{\tau}_{opt}) = 3s\bar{\tau}_{opt}^2 + 2a^2\bar{\tau}_{opt} > 0$ , since all variables are positive.

Then Thm. 2 applies and there exists a function  $\tau(\pi)$  such that  $F(\pi, \tau_{opt}) = 0 \iff \tau_{opt} = \tau(\pi)$ , with  $\pi$  in some open neighbourhood of  $\bar{\pi}$ . In fact, since we did not pose constraints on  $(\bar{\pi}, \bar{\tau}_{opt})$ , we can state that such a function is defined for all  $\pi \in \mathbb{R}_+$ . The two cases for  $\pi$  are studied independently.

$\pi = s$  By Thm. 2, the first derivative of  $\tau(\pi) = \tau(s)$  is

$$\tau'(s) = -\frac{F_s(s, \tau(s))}{F_{\tau}(s, \tau(s))} = -\frac{\tau(s)^2}{3s\tau(s) + 2a^2} \quad (26)$$

We conclude that  $\tau'(s) < 0 \forall s \in \mathbb{R}_+$ , namely,  $\tau_{opt}$  is strictly decreasing with  $s$ .

$\pi = a^2$  The first derivative of  $\tau(\pi) = \tau(a^2)$  is

$$\tau'(a^2) = -\frac{F_{a^2}(a^2, \tau(a^2))}{F_{\tau}(a^2, \tau(a^2))} = -\frac{\tau(a^2)}{3s\tau(a^2) + 2a^2} \quad (27)$$

We conclude that  $\tau'(a^2) < 0 \forall a \in \mathbb{R}$ , namely,  $\tau_{opt}$  is strictly decreasing with  $a^2$  - regardless of sign( $a$ ).

## REFERENCES

- [1] D.P. Bertsekas. *Dynamic Programming and Optimal Control, Vol. I*. Athena Scientific, 2005.
- [2] L. Blazovics, K. Csorba, B. Forstner, and C. Hassan. Target tracking and surrounding with swarm robots. In *2012 IEEE 19th International Conference and Workshops on Engineering of Computer-Based Systems*, pages 135–141, April 2012.
- [3] V.S. Borkar and S.K. Mitter. LQG control with communication constraints. *Comm., Comp., Control, and Signal Processing*, pages 365–373, 1997.
- [4] Axel Brkle, Florian Segor, and Matthias Kollmann. Towards autonomous micro uav swarms. *Journal of Intelligent and Robotic Systems*, 61:339–353, 03 2011.
- [5] L. Carlone and S. Karaman. Attention and anticipation in fast visual-inertial navigation. In *IEEE Intl. Conf. on Robotics and Automation (ICRA)*, pages 3886–3893, Singapore, May 2017. extended arxiv preprint: 1610.03344 .
- [6] L. Carlone and S. Karaman. Attention and anticipation in fast visual-inertial navigation. *IEEE Trans. Robotics*, 2018. arxiv preprint: 1610.03344, .
- [7] Sandeep Chinchali, Apoorva Sharma, James Harrison, Amine Elhafsi, Daniel Kang, Evgenya Pergament, Eyal Cidon, Sachin Katti, and Marco Pavone. Network offloading policies for cloud robotics: a learning-based approach. *arXiv e-prints*, page arXiv:1902.05703, Feb 2019.
- [8] N. Elia and S.K. Mitter. Stabilization of linear systems with limited information. *IEEE Trans. on Automatic Control*, 46(9):1384–1400, 2001.
- [9] V. Gupta, T. Chung, B. Hassibi, and R. Murray. On a stochastic sensor selection algorithm with applications in sensor scheduling and sensor coverage. *Automatica*, 42(2):251–260, 2006.
- [10] R. I. Hartley and A. Zisserman. *Multiple View Geometry in Computer Vision*. Cambridge University Press, second edition, 2004.
- [11] K. Imagane, K. Kanai, J. Katto, and T. Tsuda. Evaluation and analysis of system latency of edge computing for multimedia data processing. In *2016 IEEE 5th Global Conference on Consumer Electronics*, pages 1–2, Oct 2016.
- [12] S.T. Jawaid and S.L. Smith. Submodularity and greedy algorithms in sensor scheduling for linear dynamical systems. *Automatica*, 61:282–288, 2015.
- [13] S. Joshi and S. Boyd. Sensor selection via convex optimization. *IEEE Trans. Signal Processing*, 57:451–462, 2009.
- [14] Faming Li, Mauricio C. de Oliveira, and Robert Skelton. Integrating information architecture and control or estimation design. *SICE Journal of Control, Measurement, and System Integration*, 1:120–128, 01 2011.
- [15] Li Fan, P. Dasgupta, and Ke Cheng. Swarming-based mobile target following using limited-capability mobile mini-robots. In *2009 IEEE Swarm Intelligence Symposium*, pages 168–175, March 2009.
- [16] B. Maag, Z. Zhou, and L. Thiele. A survey on sensor calibration in air pollution monitoring deployments. *IEEE Internet of Things Journal*, 5(6):4857–4870, Dec 2018.
- [17] G.N. Nair and R.J. Evans. Stabilizability of stochastic linear systems with finite feedback data rates. *SIAM Journal on Control and Optimization*, 43(2):413–436, 2004.
- [18] E. Nozari, F. Pasqualetti, and J. Cortés. Time-invariant versus time-varying actuator scheduling in complex networks. In *American Control Conference*, pages 4995–5000, Seattle, WA, May 2017.
- [19] NVIDIA. Nvidia jetson tx2 module specifications. <https://developer.nvidia.com/embedded/buy/jetson-tx2>, 2018.
- [20] J. Le Ny, E. Feron, and M.A. Dahleh. Scheduling Continuous-Time Kalman Filters. *IEEE Trans. on Automatic Control*, 56(6):1381–1394, 2011.
- [21] J. Le Ny and G.J. Pappas. Differentially private filtering. *IEEE Trans. on Automatic Control*, 59(2):341–354, 2014.
- [22] F. Pasqualetti, F. Drfler, and F. Bullo. Cyber-physical attacks in power networks: Models, fundamental limitations and monitor design. In *IEEE Conference on Decision and Control and European Control Conference*, pages 2195–2201, 2011.
- [23] G. Radian, Y. K. Ghazijahani, A. Saadatkhah, and V. J. Majd. Dynamic obstacle avoidance and target tracking for a swarm of robots using distributed kalman filter. In *The 3rd International Conference on Control, Instrumentation, and Automation*, pages 255–259, Dec 2013.
- [24] E. Shafieepoorfard and M. Raginsky. Rational inattention in scalar LQG control. In *IEEE Conf. on Decision and Control (CDC)*, pages 5733–5739, 2013.
- [25] S. Shalev-Shwartz, S. Shammah, and A. Shashua. On a formal model of safe and scalable self-driving cars. *ArXiv*, abs/1708.06374, 2017.
- [26] A. Suleiman, Z. Zhang, L. Carlone, S. Karaman, and V. Sze. Navion: A 2mW fully integrated real-time visual-inertial odometry accelerator for autonomous navigation of nano drones. *IEEE Journal of Solid-State Circuits*, 2018.
- [27] T. Summers and M. Kamgarpour. Performance guarantees for greedy maximization of non-submodular set functions in systems and control. *arXiv e-prints:1712.04122*, 2017.
- [28] T. Summers and J. Ruths. Performance bounds for optimal feedback control in networks. *arXiv e-prints:1707.04528*, 2017.

- 
- [29] T.H. Summers, F.L. Cortesi, and J. Lygeros. On submodularity and controllability in complex dynamical networks. *IEEE Transactions on Control of Network Systems*, 3(1):91–101, 2016.
- [30] T. Taami, S. Krug, and M. ONils. Experimental characterization of latency in distributed iot systems with cloud fog offloading. In *2019 15th IEEE International Workshop on Factory Communication Systems (WFCS)*, pages 1–4, May 2019.
- [31] T. Tanaka and H. Sandberg. SDP-based joint sensor and controller design for information-regularized optimal LQG control. In *IEEE Conf. on Decision and Control (CDC)*, pages 4486–4491, Osaka, Japan, December 2015.
- [32] S. Tatikonda and S.K. Mitter. Control under communication constraints. *IEEE Trans. on Automatic Control*, 49(7):1056–1068, 2004.
- [33] Vlasios Tsiatsis, Ram Kumar, and Mani B. Srivastava. Computation hierarchy for in-network processing. *Mobile Networks and Applications*, 10(4):505–518, Aug 2005.
- [34] V. Tzoumas, L. Carlone, G.J. Pappas, and A. Jadbabaie. Sensing-constrained LQG control. In *American Control Conference*, pages 197–202, Milwaukee, WI, June 2018. arxiv preprint: 1709.08826, .
- [35] V. Tzoumas, A. Jadbabaie, and G.J. Pappas. Sensor placement for optimal kalman filtering: Fundamental limits, submodularity, and algorithms. In *American Control Conference*, 2016.
- [36] Andrew Wichmann, Burcu Demirelli Okkalioglu, and Turgay Korkmaz. The integration of mobile (tele) robotics and wireless sensor networks: A survey. *Computer Communications*, 51, 09 2014.
- [37] Shuang Wu, Kemi Ding, Peng Cheng, and Ling Shi. Optimal Scheduling of Multiple Sensors over Lossy and Bandwidth Limited Channels. *arXiv e-prints*, page arXiv:1804.05618, Apr 2018.
- [38] R. D. Yates and S. K. Kaul. Status updates over unreliable multiaccess channels. In *2017 IEEE International Symposium on Information Theory (ISIT)*, pages 331–335, June 2017.
- [39] R. D. Yates and S. K. Kaul. The age of information: Real-time status updating by multiple sources. *IEEE Transactions on Information Theory*, 65(3):1807–1827, March 2019.
- [40] Y. Zhao, F. Pasqualetti, and J. Cortés. Scheduling of control nodes for improved network controllability. In *IEEE Conf. on Decision and Control (CDC)*, pages 1859–1864, Las Vegas, December 2016.
- [41] B. Zhou and W. Saad. Joint status sampling and updating for minimizing age of information in the internet of things. *IEEE Transactions on Communications*, pages 1–1, 2019.
- [42] S. Zilberstein. Using anytime algorithms in intelligent systems. *AI Magazine*, 17(3), 1996.